Sens Imaging
DOI 10.1007/s11220-009-0046-x

ORIGINAL PAPER

Detection of Terahertz Pulses Using a Modified Sagnac Interferometer

Benjamin Clough · David H. Hurley · Pengyu Han · Jun Liao · Rena Huang · X.-C. Zhang

Received: 14 May 2009 / Revised: 6 July 2009

Abstract We describe a time resolved, interferometric method to detect terahertz (THz) pulses based on the Sagnac geometry. A ZnTe electro-optic crystal is placed in one arm of the interferometer, and the THz-induced optical phase shift is demodulated by allowing the two arms to optically interfere. The theoretical principle behind this new method is illustrated and a detailed comparison with the traditional electro-optic sampling technique used in THz time domain spectroscopy is performed. Key features of this new method are highlighted, serving as an aid to identify where this method may be useful in future applications.

Keywords Terahertz pulse detection · Sagnac interferometer · Birefringence · Phase change · Polarization change · Electro-optic

1 Introduction

Since its advent in 1995, free-space electro-optic sampling (FSEOS) has become one of the most commonly used methods for detecting broadband THz pulses.

B. Clough · P. Han · X.-C. Zhang
Center for THz Research, Rensselaer Polytechnic Institute, Troy, NY 12180, USA

D. H. Hurley
Materials Science and Engineering Department, Idaho National Laboratory, Idaho Falls, ID 83415, USA

B. Clough · J. Liao · R. Huang · X.-C. Zhang
Electrical Computer and Systems Engineering, Rensselaer Polytechnic Institute, Troy, NY 12180, USA

X.-C. Zhang (✉)
Department of Physics and Electrical Computer and Systems Engineering, Center for Terahertz Research, Rensselaer Polytechnic Institute, Troy, NY, USA
e-mail: zhangxc@rpi.edu

Published online: 24 July 2009

FSEOS relies on the polarization rotation of an optical probe beam due to THz-induced birefringence in EO materials [1–5]. Using a related detection methodology, based on the Sagnac geometry, there exists exciting potential to measure a multitude of physical processes including those involved in THz generation and propagation. The Sagnac interferometer, first introduced in 1913, has been used for a variety of applications in optics, such as the field of picosecond acoustics [6]. The basic principle of the modified Sagnac interferometer described in this paper is to split a linearly polarized optical beam into two arms, one containing the EO crystal. The signal and reference beams of the interferometer are scanned across a time window that encompasses the time duration of the THz pulse. The paths of the interferometer are designed such that the reference beam always arrives at the EO crystal after the THz pulse, while the signal beam is phase modulated by the THz-induced electro-optic effect. After the reference and signal beams travel common reversed paths, the two beams are in phase minus a small THz-induced phase change in the EO crystal. This small phase change is reflected in the output intensity after the two arms are allowed to interfere. Using the benefit of phase matching between the optical group velocity and the THz phase velocity in ZnTe [7], along with the stability [8] and polarization-insensitive properties of this detection geometry, we present an alternative method for THz detection that uses a single THz–induced birefringent axis to delay the optical probe beam in one arm of a modified Sagnac interferometer.

2 Theory of Operation

The orientation of both the electro-optic ZnTe crystal and the THz electric field vector play an important role in determining whether the sensor is used for polarization rotation detection (PRD) or optical phase detection (OPD). PRD is the traditional technique used in EO sampling and the magnitude of induced phase retardation from the THz electric field can be written as [9]:

$$\Gamma_{\max} = \frac{2\pi d}{\lambda} n_0^3 \gamma_{41} E_{\mathrm{THz}} \tag{1}$$

where d is the interaction length, λ is the optical wavelength of the probe beam in vacuum, n_0 is the optical refractive index, E_{THz} is the electric field of the THz radiation, and γ_{41} is the electro-optic coefficient.

OPD is presented below and the electric field vectors for the signal and reference beams are analyzed as they interact with the ZnTe, quarter wave plate, and linear polarizer. The Sagnac interferometer splits the optical probe beam into two beams with perpendicular polarizations which we will refer to as E_S and E_R. E_S corresponds to vertical polarization and E_R to a horizontal polarization. For a $<1\ 1\ 0>$ -cut uniaxial ZnTe crystal, the THz electric field, index ellipsoid, eigenvalues, and eigenvectors are given by the following expressions [10]:

$$\text{THz field: } \overrightarrow{E} = \frac{E_0}{\sqrt{2}}\hat{x} + \frac{E_0}{\sqrt{2}}\hat{y} \tag{2}$$

$$\text{Index Ellipsoid: } \frac{x^2 + y^2 + z^2}{n_0^2} + 2r_{41}\frac{E_0}{\sqrt{2}}(yz + zx) \tag{3}$$

$$\text{Eigenvalues: } S_1 = \frac{1}{n_0^2}, S_{2/3} = \frac{1}{n_0^2} \pm r_{41}E_0 \tag{4}$$

$$\text{Eigenvectors: } \vec{e}_1 = [1\ 1\ 0], \vec{e}_2 = [1\ \bar{1}\ \sqrt{2}], \vec{e}_3 = [\bar{1}\ 1\ \sqrt{2}] \tag{5}$$

As seen in Fig. 1, when the THz beam enters the ZnTe (into the page) with a polarization parallel to the [1 $\bar{1}$ 0] direction, only a single birefringent axis is seen by a horizontally (x) or vertically (y) polarized optical beam traveling through the crystal. For this alignment, the THz beam imposes a change in phase of the optical probe beam without any rotation in the polarization.

Before interaction with the THz beam inside the EO crystal, the electric field of the optical signal and reference beams are represented as:

$$E_s = E_R = A \tag{6}$$

The interaction of a THz beam with the ZnTe crystal introduces refractive index variation along $\mathbf{e_2}$ and $\mathbf{e_3}$. The new refractive indices are:

$$n_{e_2} = n_0 - \frac{1}{2}n_0^3 r_{41}E_{\text{THz}} \tag{7}$$

$$n_{e_3} = n_0 + \frac{1}{2}n_0^3 r_{41}E_{\text{THz}} \tag{8}$$

where n_{e_2} and n_{e_3} are refractive index along the new principal axes of $\boldsymbol{e_2}$ and $\boldsymbol{e_3}$, respectively, n_0 is the unperturbed index of refraction, $\boldsymbol{r_{41}}$ is the relevant electro-optic tensor component, and $\boldsymbol{E_{\text{THz}}}$ is the electric field of the THz beam. Letting $\Delta\phi$ represent the change in optical phase imposed by the THz beam:

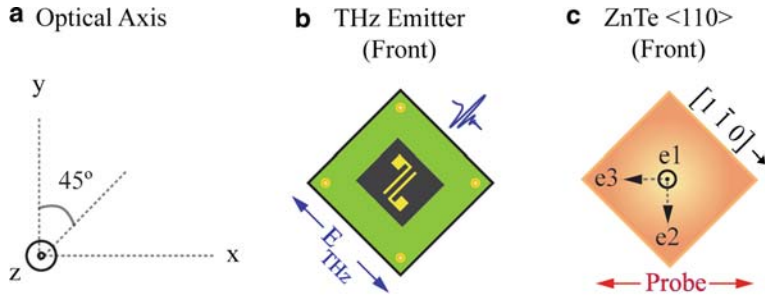

Fig. 1 **a** Optical axis of the system with optical beam propagating along the *z* axis. **b** Front view of 150 micron gap photoconductive dipole antenna (*PCDA*) emitting THz pulses polarized at 45° to the optical axis. **c** THz field induces changes of refractive index along e_2 and e_3 axes in the ZnTe crystal, which are the new principal axes. When the optical probe beam is polarized along e_2, it experiences only phase retardation, but not birefringence

$$\Delta\phi = \frac{\omega n_0^3 r_{41} E_{\mathrm{THz}} l}{2c} = \frac{\delta\Gamma}{2} \tag{9}$$

where ω is the circular frequency of the optical signal beam, l is the crystal length, and c is the speed of light in a vacuum. The signal and reference beams following interaction with the THz inside the EO crystal are given by:

$$E_{\mathrm{S}} = Ae^{-i\Delta\phi},\ E_{\mathrm{R}} = A \tag{10}$$

After the signal and reference beam pass through the quarter wave plate (see Fig. 2), the electric field of the signal and reference beams are given by:

$$E_{\mathrm{S}} = Ae^{-i\delta\Gamma/2}, E_{\mathrm{R}} = Ae^{i\pi/2} \tag{11}$$

After passage through the linear polarizer oriented at 45° from the optical axis, the components of the electric field with the polarization vector aligned with the linear polarizer's transmission axis (+45) and perpendicular to the transmission axis (−45) are given by:

$$E_{+45} = \frac{A}{\sqrt{2}}\left[e^{-i\delta\Gamma/2} + e^{i\pi/2}\right] \tag{12}$$

$$E_{-45} = \frac{A}{\sqrt{2}}\left[e^{-i\delta\Gamma/2} - e^{i\pi/2}\right] \tag{13}$$

The intensity of these two components is approximated by:

$$I_{+45} = \frac{A^2}{2}[1 + \delta\Gamma/2]^2 \tag{14}$$

$$I_{-45} = \frac{A^2}{2}[1 - \delta\Gamma/2]^2 \tag{15}$$

The process by which the in phase perpendicular components of the linear polarization are made to interfere is referred to as phase demodulation and is shown in Fig. 2.

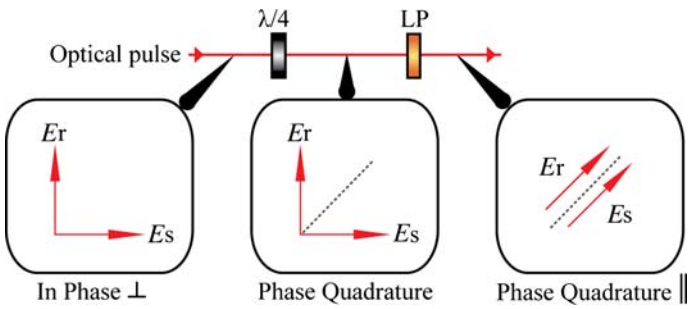

Fig. 2 A quarter wave plate and linear polarizer (*LP*) are used in the process of phase demodulation. In phase ⊥ linearly polarized optical beams E_{R} and E_{S} are set to quadrature phase (*circular*) and then through a linear polarizer to interfere. The quarter wave plate allows us to bias the intensity output to half of the maximum for sensing of the bipolar THz pulse

3 Experimental Setup and Results

A Ti:sapphire laser (Mira 900) having an 800 nm center wavelength, and <200 fs pulse duration (FWHM) with a 76 MHz repetition rate, is fed through a half wave plate to allow control over pump and probe power. The beam is split into two paths using a cubic polarizing beam splitter (PBS) as in typical pump probe measurements [11]. A 25 mm time delay stage is used in the pump arm to adjust temporal overlap of the THz and optical pulse in the birefringent ZnTe crystal. A 30 mW optical pump beam is focused onto a 150 micron gap spacing photoconductive dipole antenna (PCDA) rotated to 45° about the optical axis to generate the broadband THz. The THz signal is modulated at 30 kHz using a TTL-switched high-voltage modulator with 130 V (peak–peak) between the PCDA electrodes. A 30 mW probe beam is again split into two paths forming the arms of the Sagnac interferometer. The reference beam mentioned previously takes path (a) while the signal beam takes path (b) as indicated in Fig. 3.

Path (a) begins at PBS1, travels through the PBS2 and the quarter wave plate. After passing through the quarter wave plate a second time, the polarization is rotated from "p" to "s". It is then reflected downward by PBS2, focused through the ZnTe and indium tin oxide (ITO) glass by L2, and recollimated by L1 to meet back up with its initial origin. Both L1 and L2 have a focal length of 86.3 mm. Path (b) begins with the optical beam reflected downward by PBS1, focused by lens L1 through the ITO and ZnTe, and again collimated with L2. It is then reflected by PBS2, and sent through the quarter wave plate twice to allow for polarization change from "s" to "p". It is now let through PBS2 to meet back up with its initial origin. The delay stage is adjusted so that the path (b) pulse has interaction with the THz pulse, while path (a) does not since the THz pulse will have already passed through the ZnTe by the time the path (a) pulse enters the crystal.

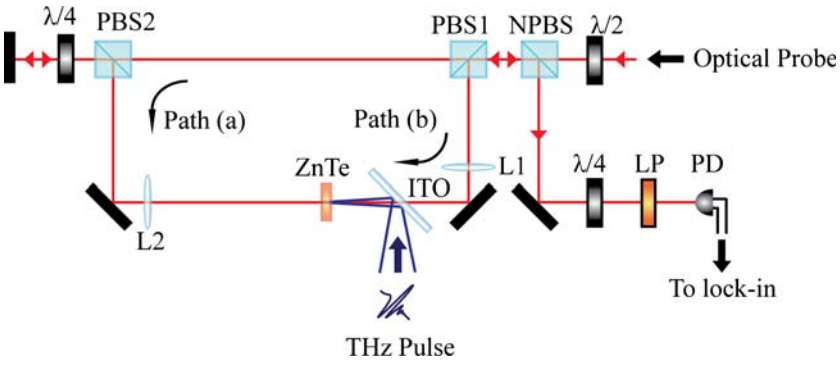

Fig. 3 Experimental layout for detection of THz pulses using a Sagnac interferometer. A THz-induced change in refractive index along the ZnTe vertical and horizontal directions keeps the optical probe beam from rotating in polarization while creating a phase delay. This small phase delay is detected by a change in constructive interference between the two interferometer optical beams E_R and E_S which take paths (a) and (b) respectively. The non-polarizing beam splitter (NPBS) is used to extract the signal and reference beam from the system once they have each traversed a common path through the interferometer

The THz emission from the PCDA is collimated by a 2" diameter 3" effective focal length (EFL) off-axis parabolic mirror (OAPM) and once again focused by a 2" diameter 4" EFL OAPM. The ITO pellicle reflects the THz while it allows the optical probe beam to pass through. The time delay stage is adjusted so the THz and optical probe pulse (E_S) travel collinearly through the 1-mm ZnTe crystal. A phase delay is created in one arm of the interferometer due to a THz-induced refractive index change in the ZnTe. In order to use optical phase detection, it is important that both the PCDA and the ZnTe are rotated by 45° such that the THz-induced principal axis in the ZnTe will delay the optical probe beam (E_S) without altering its polarization state. This condition will only be satisfied when the new principal axes are set up along the horizontal (x) and vertical (y) components of the <1 1 0> cut ZnTe (refer to Fig. 1b above). Once both optical beams path (a) and (b) recombine at PBS1, they travel to the non-polarizing beam splitter (NPBS) where the two perpendicularly-polarized optical signals E_R and E_S are extracted for detection. Without any THz influence, both E_R and E_S travel through the biasing quarter wave plate where one component is lagged by $\pi/2$ creating a circular polarization. When the THz causes a phase delay in the E_S component, the linearly decomposed components of both E_R and E_S selected by the linear polarizer also experience this phase delay, directly affecting the interference between the two of them and therefore the resulting output intensity.

The quarter wave plate preceding the linear polarizer (LP) is used to adjust the phase between the two optical beams E_R and E_S, such that the intensity due to constructive interference at the output is exactly half of the maximum. This allows for a maximum intensity swing in either direction taking into account the bipolar nature of the THz electric field. When the THz changes the index of refraction in the ZnTe, it slightly increases the time for the pulse to travel through path (b). A change in the path (b) distance results in constructive or destructive interference and a corresponding increase or decrease in intensity at the photodiode (PD). The small intensity fluctuation can be detected using balanced detection with the initial NPBS reflection (attenuated) and a pair of photodiodes to further reduce common laser noise in the system.

The normalized time domain waveforms and corresponding spectrum acquired using this interferometric technique are shown in Fig. 4 along with a comparison to the THz waveform obtained by free space electro-optic sampling. Acquisition of the electro-optic sampling data was made the same day using the traditional THz time domain spectroscopy geometry [11]. The EO data were taken with the same parameters used in the interferometer setup for a fair comparison. The probe power was adjusted to compensate for losses associated with additional optics in the interferometer experimental setup. A single scan using 100 ms lock-in time constant was used while stepping the delay stage in 4 micron steps. From Fig. 4, we can see that the two methods produce comparable results although one is detecting a rotation in polarization while the other is detecting a change in phase.

4 Discussion

The THz pulse detected using Sagnac interferometry in Fig. 4 is comparable with that obtained using traditional EO sampling. The small differences may be

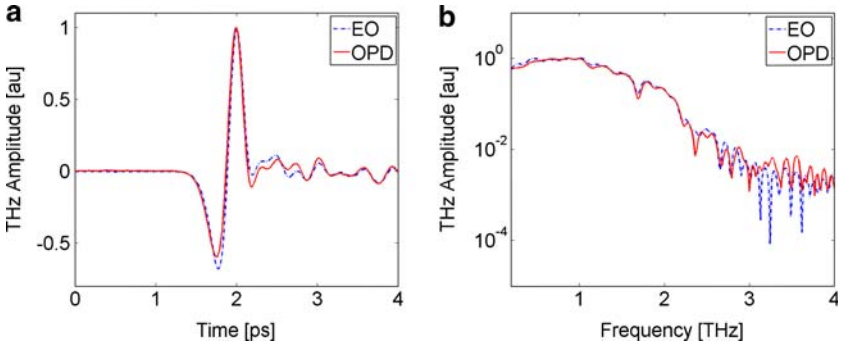

Fig. 4 **a** Normalized time domain waveforms and **b** spectrum for THz detection using optical phase detection (*OPD*) compared with the traditional EO sampling. EO data were collected using typical THz time domain spectroscopy geometry

Table 1 Features of THz detection using polarization rotation and optical phase detection methods

Feature	Electro-optic sampling	Sagnac interferometry
Parameter detected	Optical polarization rotation	Optical phase delay
No. of probe beams	1	2
Optical probe beam direction relative to THz direction	Collinear	Collinear and counter-collinear

attributed to slightly different alignments of the THz and optical probe beams between the EO and interferometer experimental setups. It is also possible that the residual birefringence in the ZnTe along axis e_3 (when the ZnTe is rotated to 45°) differs from along [1 $\bar{1}$ 0] so that the bias is slightly different from $\pi/2$.

Table 1 serves to highlight some key features that distinguish between optical phase detection used in the Sagnac interferometer, and polarization rotation detection used in free-space electro-optic sampling.

Because of fundamental differences compared with the more conventional EO technique [12], the Sagnac interferometry approach may provide additional latitude in future THz detection schemes. For example, taking advantage of the interferometer's common path design, it may be possible to develop a real-time common-mode-rejection system that would reduce undesirable water absorption lines in the spectrum and increase SNR.

5 Conclusions

An alternative terahertz detection method using Sagnac interferometry has been demonstrated. By analyzing the electro-optic properties of the ZnTe crystal, we have shown that proper orientation of the crystallographic indices and the THz electric field vector introduces a phase delay in the optical probe beam without

rotating its polarization. Using a Sagnac interferometer, we have detected the coherent time domain THz pulse, which is comparable to the one obtained by the conventional electro-optic detection method in both temporal waveforms and spectra. The optical signal and reference electric field vectors E_S and E_R have been theoretically analyzed as they propagate through the experimental setup, leading to expressions for the optical output intensity as a function of THz-induced phase change between E_S and E_R. Finally, features of both detection methods have been compared to encourage future insight into applications of the Sagnac interferometric technique.

Acknowledgments This work was sponsored by the U.S. Department of Energy to the Idaho National Laboratory Explosives Detection Research Program, operated by Battelle Energy Alliance, LLC. under DOE Idaho Operations Office Contract DE–AC07-05ID14517.

References

1. Wu, Q., & Zhang, X.-C. (1995). Free-space electro-optic sampling of terahertz beam. *Applied Physics Letters, 67*, 3523.
2. Jepsen, P. U., Winnewisser, C., Schall, M., Schyja, V., Keiding, S. R., & Helm, H. (1996). Detection of THz pulses by phase retardation in lithium tantalate. *Physical Review. E, 53*(4), R3052–R3054.
3. Nahata, A., Auston, D. H., Heinz, T. F., & Wu, C. (1996). Coherent detection of freely propagating terahertz radiation by electro-optic sampling. *Applied Physics Letters, 68*(2), 150–152.
4. Bakker, H. J., Cho, G. C., Kurz, H., Wu, Q., & Zhang, X.-C. (1998). Distortion of terahertz pulses in electro-optic sampling. *Journal of the Optical Society of America. B, Optical Physics, 15*, 1795–1801.
5. Wu, Q., & Zhang, X.-C. (1996). Design and characterization of traveling-wave electrooptic terahertz sensors. *IEEE Journal of Selected Topics in Quantum Electron, 2*, 693–700.
6. Hurley, D. H., & Wright, O. B. (1999). Detection of ultrafast phenomena by use of a modified Sagnac interferometer. *Optics Letters, 24*, 1305–1307.
7. Wu, Q., Litz, M., & Zhang, X.-C. (1996). Broadband detection capability of ZnTe electro-optic field detectors. *Applied Physics Letters, 68*, 2924–2926.
8. Ezekiel, S., & Arditty, H. J. (Eds.). (1982). *Fiber-optic rotation sensors and related technologies*. Berlin: Springer.
9. Saleh, B. E. A., & Teich, M. C. (2007). *Fundamentals of photonics* (2nd ed ed.). Hoboken, New Jersey: Wiley.
10. Namba, S. (1961). Electro-optical effect of zincblende. *Journal of the Optical Society of America, 51*, 76–79.
11. Ferguson, B., & Zhang, X.-C. (2002). Materials for terahertz science and technology. *Nature Materials, 1*, 26–33.
12. Wu, Q., & Zhang, X.-C. (1997). Free-space electro-optics sampling of mid-infrared pulses. *Applied Physics Letters, 71*, 1285–1286.